# The Wheat 55K SNP-Based Exploration of Loci for Spikelet Number Per Spike from a Tetraploid Wheat (*Triticum turgidum* L.) Recombinant Inbred Line Population derived from a Chinese Landrace 'Ailanmai' and a Wild Emmer Accession

Ziqiang Mo[1, +], Jing Zhu[1, +], Jiatai Wei[1], Jieguang Zhou[1], Qiang Xu[1], Huaping Tang[1], Yang Mu[1], Qiantao Jiang[1], Yaxi Liu[1], Guoyue Chen[1], Jirui Wang[1], Pengfei Qi[1], Zhien Pu[2], Guangdeng Chen[3], Yuming Wei[1], Youliang Zheng[1], Xiujin Lan[1, *], Jian Ma[1, *]

[1]State Key Laboratory of Crop Gene Exploration and Utilization in Southwest China, Triticeae Research Institute, Sichuan Agricultural University, Chengdu, 611130, China

[2]College of Agronomy, Sichuan Agricultural University, Chengdu, 611130, China

[3]College of Resources, Sichuan Agricultural University, Chengdu, 611130, China

[+] Contributed equally to this work.

*Authors for correspondence:

Dr. Jian Ma, E-mail: jianma@sicau.edu.cn

Dr. Xiujin Lan, E-mail:lanxiujin@163.com

**Abstract**

Increasing wheat yield is essential in solving the global food shortage. The spikelet number per spike (SNS) is a primary factor that determines the kernel number per spike which has a great effect on wheat yield. Modern wheat breeding methods reduce the genetic diversity among cultivars, leading to a detrimental effect on future wheat production. It is, therefore, necessary to explore new genetic resources for SNS to increase wheat yield. A tetraploid landrace 'Ailanmai' × wild emmer wheat recombinant inbred line (RIL) population was used to construct a high-density genetic map using the wheat 55K single nucleotide polymorphism (SNP) array. The linkage map revealed that 94.83% (6204) of the mapped markers had consistent genetic and physical chromosomal locations. Fourteen quantitative trait loci (QTL) for SNS, explaining 4.23-27.26% of the phenotypic variation, were identified. *QSns.sau-AM-2B.3* and *QSns.sau-AM-3B.2* were detected as the major and novel QTL with a large cumulative effect that increased SNS by 17.47%. Some development-related genes within the physical intervals of *QSns.sau-AM-2B.3* and *QSns.sau-AM-3B.2* were predicted to participate in spikelet growth, thereby affecting SNS. Genetic associations between SNS and other agronomic traits such as a significant and positive correlation between SNS and thousand kernel weight (TKW) were detected and analyzed. QTL analysis was also performed for other spike-related traits, including spike length (SL), kernel number per spike (KNS), kernel number per spikelet (KNL), and spike density (SD). *QSns.sau-AM-2B.3* was co-located with *QSl.sau-AM-2B* in the interval between *AX-111626925* and *AX-111588559.* Similarly, *QKns.sau-AM-5B.1* was co-related with *QKnl.sau-AM-5B.2* in the region between *AX-108760512* and *AX-110180251*. This study demonstrates the feasibility of wheat 55K SNP array in genetic mapping of tetraploid wheat population and shows the potential application of wheat related

species in wheat improvement programs.

**Keywords:** Tetraploid wheat, high-quality genetic map, spikelet number per spike, QTL mapping, genetic correlations, potential application

## Introduction

Wheat (*Triticum* sp.) is among the most widely planted crops globally that provide about 20% of the calories consumed by humans (http://www.fao.org/faostat). Breeding high-yield wheat cultivars is a sustainable approach to meet the demands of a growing human population. Wheat yield is determined by spike number per unit area (SNPA), kernel number per spike (KNS), and kernel weight (KW). KNS is jointly determined by the spikelet number per spike (SNS) and the kernel number per spikelet (KNL). SNS depends on the number of lateral spikelets produced before the spike meristem transitions to the terminal spikelet. It is a complex quantitative trait greatly affected by genetic and environmental factors (Gao et al., 2019; Kuzay et al., 2019). Therefore, dissecting the genetic mechanism of SNS at the QTL level can provide more insights into the role of SNS in yield formation (Wang et al., 2018; Ma et al., 2019a; Yao et al., 2019; Chen et al., 2020).

A few genes related to spikelet number and morphology have been reported. For example, the *WHEAT FRIZZY PANICLE* (*WFZP*) gene encodes a member of the APETALA2/ethylene response transcription factor (AP2/ERF) family, which influences the supernumerary spikelet trait in common wheat (Dobrovolskaya et al., 2015). Regulatory expression of the two pivotal flowering genes, *Photoperiod-1* (*Ppd-1*) and *FLOWERING LOCUS T* (*FT*), increases the number of fertile spikelets (Boden et al., 2015). The inflorescence growth rate and the development of paired spikelets are controlled by the *TEOSINTE BRANCHED1* (*TB1*) expression level (Dixon et al., 2018). Similarly, the ortholog of the rice *APO1*, *WHEAT ORTHOLOG OF APO1* (*WAPO1*) affects the spikelet number (Kuzay et al., 2019). Overexpression of *TaTFL-2D* increases the number of spikelets and florets (Wang et

al., 2017). The transcription factor *TaNAC67* participates in the regulation of spike length and spikelet number (Zhang et al., 2019).

More loci for SNS should thus be identified and utilized owing to its important role in yield formation. Nonetheless, modern wheat breeding reduces the genetic diversity among cultivars, thus adversely affecting wheat yield (Tanksley and McCouch, 1997; Cavanagh et al., 2013; Sthapit et al., 2020). Notably, the numerous untapped genetic resources from wheat related species may effectively solve future wheat production challenges (Reynolds et al., 2011; Longin and Reif, 2014; Martínez-Moreno et al., 2020).

As the progenitor of modern cultivated tetraploid and hexaploid wheat, wild emmer wheat (*T. turgidum* subsp. *dicoccoides*) is the secondary gene source of common wheat. It is resistant to various diseases and possesses important agronomic traits, thereby playing a significant role in wheat breeding (Tanksley and McCouch, 1997; Xie and Nevo, 2008; Yu et al., 2020). For example, *Yr15* derived from wild emmer wheat confers resistance to yellow rust (Klymiuk et al., 2018). The reduced-function allele *GNI-A1* increases the number of fertile florets per spikelet (Sakuma et al., 2019). Cognizant of this, exploiting the genetic resources of wild emmer wheat is crucial in solving the existing bottlenecks in wheat breeding. Wheat landraces are also primary materials for wheat improvement and breeding (Lin et al., 2020). They are precious resources preserved under long-term natural selection and human intervention with strong adaptability to local environmental conditions and high production potential because of their peculiar gene resources (Lopes et al., 2015; Crossa et al., 2016).

In the current research, a high-quality genetic map was constructed based on a tetraploid wheat population developed from the cross between a Chinese landrace ‘Ailanmai’ and a wild emmer wheat accession using the wheat 55K SNP array. The QTL for SNS was subsequently identified based on the genetic map and phenotype data measured from multiple environments. Candidate genes in the intervals of the

wild emmer genome (Avni et al., 2017) harboring major and stably expressed SNS QTL were predicted. The genetic correlations between SNS and nine other agronomic traits were also detected and analyzed. These traits included plant height (PH), anthesis date (AD), productive tiller number (PTN), spike length (SL), spike extension length (SEL), kernel number per spike (KNS), kernel number per spikelet (KNL), spike density (SD), and thousand kernel weight (TKW). This study broadens the understanding of the genetic associations between agronomic traits and the utilization potential of wheat related species in common wheat improvement.

## Materials and Methods

### Plant Materials

A tetraploid wheat population (AM population) containing 121 $F_8$ recombinant inbred lines (RILs, including parents) derived from a Chinese landrace 'Ailanmai' (AL, *T. turgidum* L. cv. Ailanmai, 2n=28, AABB) and a wild emmer accession (LM001, *T. turgidum* subsp. *dicoccoides*) were used in this study. AL and LM001 have been widely used as breeding parents. A RIL population between them was developed to identify favorable alleles for specific traits to speed up their breeding utilization. AL and LM001 were collected and preserved by Triticeae Research Institute, Sichuan Agricultural University. Their spikes are shown in Figure 1.

### Trait Measurement and Data Analysis

AM RILs trait measurements were collected in six environments: Chongzhou (103° 38′ E, 30° 32′ N) in 2017, 2018, 2019, and 2020 ($E_1$, $E_2$, $E_3$, and $E_4$), Wenjiang (103° 51′ E, 30° 43′ N) in 2020 ($E_5$), and Ya'an (103° 0′ E, 29° 58′ N) in 2020 ($E_6$).

Field experiments were carried out in a randomized complete block design with two replications. The experiments were managed following the conventional practices of wheat production. Each plot for a single line was space-planted (0.1-m) in a single

1.5-m row with a 0.3-m of row spacing (Ma et al., 2019b). The partial agronomic traits were measured using a method described by Liu et al. (2020a). SNS was measured by calculating the spikelet number of the main-spike; PH was determined by the distance from the soil surface to the tip of the main-spike (excluding awns); PTN was represented by the number of productive tillers per plant; SL was counted by the length from the base to the tip of the main-spike (excluding awns); KNS was measured as the kernel number of the main-spike; SD was calculated by dividing the SNS by SL; TKW was represented by 1000 times of the average kernel weight of main-spike. AD was the number of days between sowing and half of the plants flowering (Ma et al., 2019a), while SEL was measured as the distance between the base of the spike and the petiole of the flag leaf (Tao et al., 2019). KNL was the ratio of KNS to SNS (Peng et al., 2001). Measurements were taken from at least three randomly selected plants with a consistent growth status. Their averages were used for the subsequent analyses. The environmental information of surveyed agronomic traits is listed in Supplementary Table 1.

The IBM SPSS Statistics 25 (http://en.wikipedia.org/wiki/SPSS) was used to analyze the phenotypic data, including Pearson's correlation, frequency distribution, standard error, and the Student's *t*-test ($P < 0.05$). The broad-sense heritability ($H^2$) and best linear unbiased prediction (BLUP) of the agronomic traits from different environments were calculated using SAS version 8.0 (https://www.sas.com).

**Construction of the Genetic Map**

High-quality genomic DNA was isolated from fresh leaves of AM RILs using the Plant Genomic DNA Kit (Tiangen Biotech, Beijing, China). The DNA of each line was subsequently genotyped by CapitalBio Technology (Beijing, China) using the wheat 55K SNP array.

The genetic map was constructed following the methods described by Liu et al. (2018). Markers from the Poly High-Resolution group in the wheat 55K SNP array

were retained for subsequent analysis. However, markers showing a minor allele frequency (< 0.3) among the AM RILs were removed. Markers from the D genome were also deleted. The parameters 'Distortion value' and 'Missing rate' were set as 0.01 and 20%, respectively, based on their separation patterns in AM RILs. The remaining SNP markers were analyzed using the BIN function of IciMapping 4.1 (http://www.isbreeding.net/). Only the markers with 'deleted = 0' from each bin (bin marker) were selected to construct genetic maps. The bin markers were sorted using the Kosambi mapping function in JoinMap 4.0 (https://www.kyazma.nl/index.php/JoinMap/) and the minimum LOD value was set as 5. The genetic maps were drawn using MapChart 2.3.2 (http://www.biometris.nl/uk/Software/MapChart/). The syntenic relationships between the genetic and physical maps of the bin markers were further presented using the Strawberry Perl 5.24.0.1 (http://perldoc.perl.org/perlintro.html).

**QTL Analysis**

QTL analysis was performed using the inclusive composite interval mapping (ICIM) in the Biparental Populations (BIP) module of IciMapping 4.1, with the minimal LOD score set as 2.5. The QTL-by-Environment interaction was analyzed using the multi-environment trials (MET) pattern of IciMapping 4.1. The QTL was then named following the Genetic Nomenclature provision (http://wheat.pw.usda.gov/ggpages/wgc/98/Intro.htm). In the naming system, 'Sau' represented 'Sichuan Agricultural University'. The RILs' name 'AM' was also added to the QTL's name to distinguish them from others reported previously.

Sequences of the SNP markers were blasted against the wild emmer (https://www.dropbox.com/sh/3dm05grokh10nbv/AAC3wv1YmAher8fY0srX3gX9a?dl=0%22) (Avni et al., 2017) and common wheat genotype 'Chinese Spring' (CS) genomes (IWGSC RefSeq v1.0; https://urgi.versailles.inra.fr/download/iwgsc/) to identify their physical positions. Predicted genes mapped between the flanking markers were obtained from the Triticeae Multi-omics Center

(http://202.194.139.32/), and functionally annotated using UniProt (http://www.uniprot.org/).

## Results

### SNP Markers and Genetic Map

The Affymetrix Company suggested that the high probability probes from the Poly High-Resolution group should be reserved. Thus, markers from the A and B genomes with minor allele frequency (> 0.3) among the SNP markers from the Poly High-Resolution group were retained. Finally, 7901 SNP markers were classified into 1192 bins, and one marker from each bin was screened to construct the genetic map. The linkage analysis results revealed that 1150 bin markers were mapped on 15 genetic maps. Subsequently, 6542 co-segregated SNP markers were integrated into the genetic map based on the bin information.

The 1150 bin markers were mapped on 15 linkage groups spanning 2411.78 cM in the 14 chromosomes of tetraploid wheat (Table 1 and Supplementary Table 2). One linkage group was constructed for each chromosome except chromosome 3B, which had two. The average distance of bin markers ranged between 1.09 cM (4B) and 3.64 cM (3B2), with an average density of one bin marker per 2.10 cM. The lengths of genetic maps ranged between 49.69 cM (3B1) and 225.06 cM (5A). Among the 1150 bins, 450 bins contained only one marker (Supplementary Table 3). The largest bin contained 561 markers on chromosome 2A.

The number of mapped markers (including bin markers and co-segregated markers) ranged between 37 on chromosome 3B1 and 944 on chromosome 2A (Table 1 and Supplementary Table 3). Notably, 56% and 44% of the mapped markers were distributed on A and B genomes, respectively.

### Comparison of Genetic and Physical Maps

The sequences of the 6542 mapped markers were blasted against wild emmer and CS reference genomes to identify their physical positions. The genetic and physical chromosomal locations of the 1150 bin markers in the wild emmer genome were subsequently compared (Figures 2, 3 and Supplementary Table 3). Among them, 35 (3.04%) showed inconsistent chromosomal locations, 49 (4.26%) were mapped on unknown chromosomes, while the remaining bin markers (1066, 92.70%) were well matched.

Similarly, the genetic and physical chromosomal locations of the 6542 mapped markers in the wild emmer genome were compared (Supplementary Table 3 and Supplementary Figure 1). Among them, 125 (1.91%) markers were mapped on unknown chromosomes, while 213 (3.26%) markers were mapped on inconsistent chromosomal locations. The genetic and physical location of the remaining markers (6204, 94.83%) was identical and had roughly the same SNP order.

Among the 6542 mapped markers, the physical chromosomal locations of 295 (4.51%) markers were inconsistent on wild emmer and CS reference genomes (Supplementary Table 3). However, the remaining markers (6247, 95.49%) showed good consistencies.

**Phenotypic Variation**

The SNS of AL and LM001 in six environments ranged between 25.00 and 27.00, and 23.33 and 26.00, respectively. That of AM RILs ranged between 15.33 and 34.00 (Table 2). There were no significant differences between the two parental lines in multiple environments. However, continuous variation and bidirectional transgressive segregation of the SNS was observed in the RIL population. These results suggested that it was feasible to analyze the SNS loci in the current tetraploid RIL population.

The broad-sense heritability ($H^2$) of SNS was 0.82 (Table 2), indicating that the SNS trait of the AM population was mainly controlled by genetic factors rather than

environmental factors. There were significant Pearson's correlations in the SNS of the six environments ranging between 0.500 and 0.761 (Table 3). The frequency distribution of SNS in multiple environments indicated that it was polygenically inherited (Supplementary Figure 2).

**Pearson's Correlations between SNS and other Agronomic Traits**

Pearson's correlations were analyzed between SNS and nine other agronomic traits based on the BLUP values (Table 4). SNS was significantly and positively correlated with PH, AD, SL, SEL, KNS, SD, and TKW. However, SNS was not significantly correlated with PTN and KNL.

**Analysis of QTL Associated with SNS**

A total of fourteen QTL for SNS were identified in the AM RIL population. They were distributed on chromosomes 1A (1 QTL), 3A (1), 5A (2), 6A (1), 2B (3), 3B (2), 4B (1), 5B (2), and 6B (1), with LOD scores ranging between 2.53 and 13.28. They explained 4.23-27.26% of the phenotypic variation (Table 5). The positive alleles of eight QTL were from AL while LM001 contributed the remaining six. Four QTL were detected in at least two environments, while the other ten were detected in a single environment (Table 5).

*QSns.sau-AM-5A.2* was identified in two environments. It spanned 19.10 cM between *AX-108790581* and *AX-111596791*, accounting for 6.69-14.34% of the phenotypic variation (Table 5). AM RILs were divided into two categories based on the genotype of the flanking markers of *QSns.sau-AM-5A.2*. The SNS of the lines with the positive allele was significantly higher than that of lines with the negative allele from *QSns.sau-AM-5A.2* (Figure 4a).

*QSns.sau-AM-2B.3* was stably identified in all environments, explaining 9.64-27.26% of the phenotypic variation. It was located in a 1.79 cM region between *AX-111626925* and *AX-111588559* (Table 5). The additive effect of

*QSns.sau-AM-2B.3* was negative, indicating that the increasing SNS alleles were contributed by LM001 (Table 5 and Figure 4b).

*QSns.sau-AM-3B.1* and *QSns.sau-AM-3B.2* were detected in two and four environments, respectively. They explained up to 18.06% and 13.74% of the phenotypic variation (Table 5). The positive alleles of *QSns.sau-AM-3B.1* and *QSns.sau-AM-3B.2* were from AL. Lines containing the positive allele of either *QSns.sau-AM-3B.1* or *QSns.sau-AM-3B.2* had a higher SNS than those containing the negative allele (Figure 4c, d).

The QTL-by-Environment interaction analysis identified 42 QTL (Supplementary Table 4). Nine of them, including *QSns.sau-AM-5A.2*, *QSns.sau-AM-2B.3*, *QSns.sau-AM-3B.1*, and *QSns.sau-AM-3B.2*, were the same as detected in individual environment analysis, indicating that they were stably expressed for SNS.

**Effects of Major SNS QTL on Increasing SNS**

In this study, two major and stably expressed QTL (*QSns.sau-AM-2B.3* and *QSns.sau-AM-3B.2*) were identified for SNS in more than three environments. Their effects on increasing the SNS were further revealed using the Student's *t*-test based on the genotypes of the flanking markers (Figure 5).

Compared to the lines that carried the negative alleles from two QTL, lines with the positive allele of *QSns.sau-AM-2B.3* and *QSns.sau-AM-3B.2* increased SNS significantly by 8.23% and 6.52%, respectively; their cumulative effect significantly increased SNS by 17.47%. *QSns.sau-AM-2B.3* had the largest individual effect on increasing SNS. However, there were no significant differences between the individual effects of *QSns.sau-AM-2B.3* and *QSns.sau-AM-3B.2*. The cumulative effect of major QTL increased SNS by 8.53% and 10.28%, respectively, compared to the lines that carried the positive allele from one of them.

**Effects of the Major SNS QTL on other Agronomic Traits**

AM RILs were divided into two lines containing the positive and negative alleles of two major QTL to analyze their effects on other agronomic traits (Figure 6). The cumulative effect of *QSns.sau-AM-2B.3* and *QSns.sau-AM-3B.2* significantly influenced the SL, SEL, and KNS. However, it did not significantly affect PH, AD, PTN, KNL, SD, and TKW.

**Co-location of the Major QTL for Spike-related Traits**

The QTL for SL, KNS, KNL, and SD were identified to reveal the genetic relationship between SNS and other spike-related traits (Supplementary Table 5). There were several major QTL for the corresponding traits. *QSl.sau-AM-2B* for SL was identified in three environments and located in a 1.79 cM region between *AX-111626925* and *AX-111588559*. *QKns.sau-AM-3A.2* for KNS was detected in two environments, explaining 7.48-15.29% of the phenotypic variation. *QKns.sau-AM-5B.1* for KNS spanned 0.45 cM and explained up to 16.84% of the phenotypic variation. Similarly, *QKnl.sau-AM-5B.2* for KNL explained up to 19.13% of the phenotypic variation. *QSd.sau-AM-5A.2* for SD was detected between *AX-110035703* and *AX-111076855*, accounting for 14.67-20.46% of the phenotypic variation.

Comparison of the genomic regions of the major QTL for spike-related traits revealed two co-location intervals. *QSl.sau-AM-2B* and *QSns.sau-AM-2B.3* were co-located in the interval between *AX-111626925* and *AX-111588559*, while *QKns.sau-AM-5B.1* and *QKnl.sau-AM-5B.2* were co-located in the region between *AX-108760512* and *AX-110180251* (Table 5 and Supplementary Table 5).

**Discussion**

**Exploration of the SNS Loci from Tetraploid Wheat Species Using the Wheat 55K SNP Array**

Previous studies have reported on SNS in tetraploid wheat at the QTL level. Peng et

al. (2001) identified four SNS QTL, explaining a total of 49.3% of the phenotypic variation in a wild emmer × durum wheat $F_2$ population genotyped using restriction fragment length polymorphisms (RFLP) markers. Genotyping of the durum × cultivated emmer wheat RIL population with the 9 K iSelect SNP chip identified four SNS QTL on chromosomes 1B, 3B, 7A, and 7B (Faris et al., 2014a). In the same line, a linkage map of chromosome 2A generated in the Langdon × Langdon-wild emmer wheat substitution lines population consisting of 23 simple sequence repeat (SSR) markers identified an SNS QTL, *QSpn.fcu-2A*, explaining 19.4% of the phenotypic variation (Faris et al., 2014b). SNS QTL, *QSpn.fcu-1B*, and *QSpn.fcu-5A*, have been identified in a durum × cultivated emmer wheat population genotyped using the 90K iSelect array (Sharma et al., 2019). These reports enhance our understanding of the genetic mechanism of SNS in tetraploid wheat.

Compared with the above genotyping technologies, the wheat 55K SNP array has been widely used for genotyping and QTL identification in hexaploid common wheat because it is economical and has practical characteristics (Liu et al., 2018; Ren et al., 2018; Ma et al., 2019a; Liu et al., 2020a; Liu et al., 2020b; Ma et al., 2020; Tu et al., 2021). To the author's knowledge, this is the first study to use the wheat 55K SNP array to construct the genetic linkage map of a tetraploid wheat RIL population. *QSns.sau-AM-2B.3* and *QSns.sau-AM-3B.2* were the major QTL with a large cumulative effect on increasing SNS. They have higher application potential in common wheat improvement through polymerization breeding by marker-assisted selection. These results confirm the feasibility of using a 55K SNP array developed for common wheat for genetic mapping of tetraploid wheat, thus proving its broad utilization.

**Comparison of the Major SNS QTL Identified with those of Previous Studies**

There were no significant differences for SNS detected between the parental lines in multiple environments (Table 2). The phenotypic data of SNS in the six environments showed approximately normal distribution (Supplementary Figure 2).

Two major and stably expressed QTL for SNS were identified. This phenomenon is attributed to the transgressive inheritance in progenies that result in the bidirectional segregation of SNS. Several genes controlling SNS may inhibit each other in a given parental genotype resulting in the absence of the corresponding phenotype in the parents. However, a single locus produced by genetic recombination between parental genotypes can display a conspicuous phenotype in the progenies without interference from other loci that control the same trait. The major SNS loci in the AM RIL population can thus be identified. This is not uncommon in the past studies of QTL identification based on RIL populations (Liu et al., 2020a; Shang et al., 2020; Tu et al., 2021).

Physical locations of previously identified SNS QTL on chromosome 2B and 3B in wild emmer and CS reference genomes were detected to verify whether *QSns.sau-AM-2B.3* and *QSns.sau-AM-3B.2* were novel QTL (Supplementary Table 6). *QSns.sau-AM-2B.3* was physically located on chromosome arm 2BL at 714.47-717.09 Mbp (Figure 7a). Previous studies have detected SNS QTL on chromosome arm 2BS. However, none has been reported on 2BL (Supplementary Table 6). For example, *Qspn-2007* is located on chromosome arm 2BS with the closest marker *Xgwm429* (73.62 Mbp) (Manickavelu et al., 2011). *QFsn.sdau-2B-1* is located on chromosome arm 2BS, explaining up to 28.43% of the phenotypic variation (Deng et al., 2017). Xie et al. (2015) detected three QTL for SNS on chromosome arm 2BS in an $F_5$ RIL population. Some genes regulating SNS, such as *Ppd-B1* (Mohler et al., 2004) and *WFZP-2B* (Dobrovolskaya et al., 2015), have also been detected on chromosome arm 2BS.

*QSns.sau-AM-3B.2* was physically located on chromosome arm 3BS at 62.41-65.16 Mbp (Figure 7b). Azadi et al. (2015) detected four QTL for SNS on chromosome arm 3BL. Similarly, *QSpn.fcu-3B* is located on chromosome arm 3BS at 74.28-120.61 Mbp with flanking markers *IWA3716* and *IWA6201* (Faris et al., 2014a). Cui et al. (2012) identified two QTL, *QSpn.WJ.3B.1* and *QSpn.WY.3B.1*, all

closely linked to the locus *Xgwm566* (77.72 Mbp).

Comparing the physical positions of *QSns.sau-AM-2B.3* and *QSns.sau-AM-3B.2* with those reported previously showed no overlaps with known SNS QTL, suggesting that they are probably novel QTL controlling SNS in tetraploid wheat.

**Gene Prediction in the Physical Intervals of the Major SNS QTL**

*QSns.sau-AM-2B.3* was physically located in 709.43-712.30 Mbp and 714.47-717.09 Mbp of wild emmer and CS reference genomes, respectively (Figure 7a). There were 32 and 27 predicted genes in the corresponding intervals, respectively (Supplementary Table 7). There were 18 functional orthologs among the predicted genes of *QSns.sau-AM-2B.3* (Supplementary Table 7). *QSns.sau-AM-3B.2* was located in 70.92-73.35 Mbp and 62.41-65.16 Mbp of wild emmer and CS reference genomes, respectively, with 24 functional orthologs (Figure 7b and Supplementary Table 8).

Among the orthologs, *TRIDC2BG075100* and *TRIDC3BG013290* are members of the F-box protein family. The F-box family protein plays a vital role in controlling the flowering time, floral organ development, and cell proliferation (Samach et al., 1999; Nelson et al., 2000; Xu et al., 2016). *TRIDC2BG075120* encodes an IQ-domain 32 protein that cooperates with calmodulin to regulate the basic defense response and growth of plants (Cornelia et al., 2013). *TRIDC2BG075260* encodes a serine hydroxymethyltransferase (SHMT), which is a key enzyme in plant photorespiration. Lack of SHMT cause severe growth delay and weaken the plant's resistance to abiotic stresses (Beckmann et al., 1997). *TRIDC3BG013250* and *TRIDC3BG013410* are members of the Receptor-like protein kinases (RLKs) involved in signal transduction and plant growth (Walker, 2010). All these genes play an important role in plant growth and development, potentially participating in wheat spikelet formation, thereby affecting the SNS. These results provide a foundation for subsequent works regarding fine mapping and gene cloning of major

SNS QTL.

**Significant Correlations between SNS and other Agronomic Traits**

SNS was significantly and positively correlated with PH in the present study (Table 4). This finding was consistent with that of Ajmal et al. (2009) and Wu et al. (2012). We speculate that SL is part of PH, and the taller plants have a long spike with more spikelets (Yao et al., 2011). There was a significant and positive relationship between SNS and AD (Table 4), consistent with the results of Ma et al. (2019a). It is postulated that wheat plants that take longer to flower tend to produce longer spikes with more spikelets (Shaw et al., 2013; Kamran et al., 2014; Boden et al., 2015). These results indicate that AD plays an important role in spikelet formation.

Similarly, there was a significant and positive correlation between SNS and SL (Table 4). The increase in SL requires a longer spike development stage combined with optimal temperature and light to promote spikelet germination (Rawson and Richards, 1993; Shaw et al., 2013). On the whole, floret fertility determines the KNS in wheat. More spikelets produce more fertile florets, thereby increasing the KNS (Gao et al., 2019; Sakuma et al., 2019). This reason potentially caused the SNS to be significantly and positively correlated with KNS (Table 4). Moreover, SNS was significantly and positively correlated with SD because SD is the ratio of SNS to SL (Table 4).

It is postulated that there is a negative correlation between SNS and TKW (Li et al., 2007; Ma et al., 2019a). The negative correlation is attributed to source limitations during kernel filling or more kernels with lower KW in the spike's distal positions (Quintero et al., 2018). Previous studies also suggest that SNS is negatively correlated with SEL because of competition in product assimilation between SNS and SEL (Miralles et al., 1998; Bancal, 2008; Li et al., 2020). However, these conclusions are inconsistent with the findings of this study. Herein, SNS was significantly and positively correlated with TKW and SEL (Table 4). Our further

results also revealed there were significant differences in the SEL between the two types (lines with and without the positive alleles from major QTL) (Figure 6e). It probably indicates that the loci controlling SNS play an individual role without interacting with SEL. Previous studies postulate that SEL has a special function in photosynthesis and nutrients and water storage. Therefore, a longer SEL is more conducive for ventilation and transportation of more nutrients and water to kernels (Bridgemohan and Bridgemohan, 2014; Ávila-Lovera et al., 2017), thereby increasing the KW. Thus, SNS was significantly and positively correlated with SEL and TKW in the current study.

These conclusions are vital in comprehensively understanding the complex relationships in agronomic traits, and provide new insights into wheat yield improvement.

**Co-location Regions of the QTL for Spike-related Traits**

*QSl.sau-AM-2B* was co-located with *QSns.sau-AM-2B.3*. Similarly, *QKns.sau-AM-5B.1* and *QKnl.sau-AM-5B.2* were co-located in an identical region. Generally, some QTL for pairwise traits with strong genetic correlations tend to be co-located. For example, SNS and SL (Cui et al., 2012), SNS and KNS (Zhang et al., 2009), SNS and SD (Zhang et al., 2009; Cui et al., 2012; Luo et al., 2016), SL and SD (Zhang et al., 2009; Luo et al., 2016), and SL and KNS (Zhang et al., 2009) have been mapped in the same genomic region. The co-located interval is likely involved in multiple traits with higher correlations, and a major QTL with pleiotropic effects or a QTL cluster in the same genomic region affecting various traits exist (Cui et al., 2012; Tu et al., 2021). Fine mapping or cloning of these QTL in the future can reveal their genetic mechanisms in depth. Though the genetic relationships between spike-related traits are complicated, KNS is one of the primary determinants of grain yield. Therefore, wheat breeding programs should focus on increasing SNS under moderate SD in the present study.

## Conclusion

Herein, the wheat 55K SNP array was successfully used to construct a high-quality genetic map that identified two major and novel QTL for SNS in a tetraploid wheat RIL population. The individual and cumulative effects of the major SNS QTL in increasing SNS were further revealed. Some development-related genes within the physical intervals of the major SNS QTL were also predicted. The significant correlations between SNS and other agronomic traits were evaluated, and two co-located chromosomal intervals for spike-related traits were identified. This study demonstrates the feasibility of wheat 55K SNP array in genetic mapping of tetraploid wheat and shows the potential application of wheat related species in wheat improvement programs.

## Data Availability Statement

All data generated or analyzed during this study are included in this published article and its supplementary information files, further inquiries can be directed to the corresponding author.

## Author Contributions

ZQM and JZ conducted the study and drafted this manuscript. JTW and JGZ participated in phenotype measurement and data analysis. QX and HPT helped with field work and data analysis. YM, QTJ, and YXL participated in data collection and analysis. GYC, JRW, PFQ, ZEP, and GDC did QTL analysis and manuscript revision. YMW and YLZ discussed the results and revised the manuscript. XJL guided the study and revised the manuscript. JM designed the experiments, guided the entire study, participated in data analysis, wrote and extensively revised this manuscript. All authors participated in the research and approved the final manuscript.

## Funding

This work is supported by the National Natural Science Foundation of China

(31971937 and 31970243), the Key Research and Development Program of Sichuan Province (2018NZDZX0002), the Applied Basic Research Programs of Science and Technology Department of Sichuan Province (2020YJ0140 and 2021YJ0503), the International Science and Technology Cooperation and Exchanges Program of Science and Technology Department of Sichuan Province (2021YFH0083), and the Key Projects of Scientific and Technological Activities for Overseas Students of Sichuan Province. The funders did not participate in the study design, data analysis, or preparation of the manuscript.

**Conflict of Interest**

The authors declare that they have no competing interests.

**References**

Ajmal, S., Zakir, N., and Mujahid, M. (2009). Estimation of genetic parameters and character association in wheat. *J. Agric. Biol. Sci.* 1, 15-18. doi: 10.5713/ajas.2011.10456.

Ávila-Lovera, E., Zerpa, A.J., and Santiago, L.S. (2017). Stem photosynthesis and hydraulics are coordinated in desert plant species. *New Phytol.* 216, 1119-1129. doi: 10.1111/nph.14737.

Avni, R., Nave, M., Barad, O., Baruch, K., Twardziok, S., Gundlach, H., et al. (2017). Wild emmer genome architecture and diversity elucidate wheat evolution and domestication. *Science* 357, 93-97. doi: 10.1126/science.aan0032.

Azadi, A., Mardi, M., Hervan, E.M., Mohammadi, S.A., Moradi, F., Tabatabaee, M.T., et al. (2015). QTL mapping of yield and yield components under normal and salt-stress conditions in bread wheat (*Triticum aestivum* L.). *Plant Mol. Biol. Rep.* 33(1), 102-120. doi: 10.1007/s11105-014-0726-0.

Bancal, P. (2008). Positive contribution of stem growth to grain number per spike in wheat. *Field Crop Res.* 105(1), 27-39. doi: 10.1016/j.fcr.2007.06.008.

Beckmann, K., Dzuibany, C., Biehler, K., Fock, H., Hell, R., Migge, A., et al. (1997). Photosynthesis and fluorescence quenching, and the mRNA levels of plastidic glutamine synthetase or of mitochondrial serine hydroxymethyltransferase (SHMT) in the leaves of the wild-type and of the SHMT-deficient stm mutant of *Arabidopsis thaliana* in relation to the rate of photorespiration. *Planta* 202(3), 379-386. doi: 10.1007/s004250050140.

Boden, S.A., Cavanagh, C., Cullis, B.R., Ramm, K., Greenwood, J., Jean Finnegan, E., et al. (2015). *Ppd-1* is a key regulator of inflorescence architecture and paired

spikelet development in wheat. *Nat. Plants* 1(2), 14016. doi: 10.1038/nplants.2014.16.

Bridgemohan, P., and Bridgemohan, R.S.H. (2014). Evaluation of anti-lodging plant growth regulators on the growth and development of rice (*Oryza sativa*). *J Cereals Oilseeds* 5, 12-16. doi: 10.5897/JCO14.0128.

Cavanagh, C.R., Chao, S., Wang, S., Huang, B.E., Stephen, S., Kiani, S., et al. (2013). Genome-wide comparative diversity uncovers multiple targets of selection for improvement in hexaploid wheat landraces and cultivars. *Proc. Natl. Acad. Sci. U. S. A.* 110(20), 8057-8062. doi: 10.1073/pnas.1217133110.

Chen, Z., Cheng, X., Chai, L., Wang, Z., Du, D., Wang, Z., et al. (2020). Pleiotropic QTL influencing spikelet number and heading date in common wheat (*Triticum aestivum* L.). *Theor. Appl. Genet.* 133(6), 1825-1838. doi: 10.1007/s00122-020-03556-6.

Cornelia, F., Annette, K., Stefan, H., and Petra, D. (2013). An IQ domain mediates the interaction with calmodulin in a plant cyclic nucleotide-gated channel. *Plant Cell Physiol.* 54, 573-584. doi: 10.1093/pcp/pct021.

Crossa, J., Jarquin, D., Franco, J., Perezrodriguez, P., Burgueno, J., Saintpierre, C., et al. (2016). Genomic prediction of gene bank wheat landraces. *G3-Genes Genomes Genet.* 6(7), 1819-1834. doi: 10.1534/g3.116.029637.

Cui, F., Ding, A., Li, J., Zhao, C., Wang, L., Wang, X., et al. (2012). QTL detection of seven spike-related traits and their genetic correlations in wheat using two related RIL populations. *Euphytica* 186(1), 177-192. doi: 10.1007/s10681-011-0550-7.

Deng, Z., Cui, Y., Han, Q., Fang, W., Li, J., and Tian, J. (2017). Discovery of consistent QTLs of wheat spike-related traits under nitrogen treatment at different development stages. *Front. Plant Sci.* 8, 2120. doi: 10.3389/fpls.2017.02120.

Dixon, L.E., Greenwood, J.R., Bencivenga, S., Zhang, P., Cockram, J., Mellers, G., et al. (2018). *TEOSINTE BRANCHED1* regulates inflorescence architecture and development in bread wheat (*Triticum aestivum*). *Plant Cell* 30(3), 563-581. doi: 10.1105/tpc.17.00961.

Dobrovolskaya, O., Pont, C., Sibout, R., Martinek, P., Badaeva, E., Murat, F., et al. (2015). *FRIZZY PANICLE* drives supernumerary spikelets in bread wheat. *Plant Physiol.* 167, 189-199. doi: 10.1104/pp.114.250043.

Faris, J.D., Zhang, Q., Chao, S., Zhang, Z., and Xu, S.S. (2014a). Analysis of agronomic and domestication traits in a durum × cultivated emmer wheat population using a high-density single nucleotide polymorphism-based linkage map. *Theor. Appl. Genet.* 127, 2333-2348. doi: 10.1007/s00122-014-2380-1.

Faris, J.D., Zhang, Z., Garvin, D.F., and Xu, S.S. (2014b). Molecular and comparative mapping of genes governing spike compactness from wild emmer wheat. *Mol. Genet. Genomics* 289(4), 641-651. doi: 10.1007/s00438-014-0836-2.

Gao, X., Wang, N., Wang, X., and Zhang, X. (2019). Architecture of wheat inflorescence: insights from rice. *Trends Plant Sci.* 24, 802-809. doi: 10.1016/j.tplants.2019.06.002.

Kamran, A., Iqbal, M., and Spaner, D. (2014). Flowering time in wheat (*Triticum*

*aestivum* L.): a key factor for global adaptability. *Euphytica* 197, 1-26. doi: 10.1007/s10681-014-1075-7.

Klymiuk, V., Yaniv, E., Huang, L., Raats, D., Fatiukha, A., Chen, S., et al. (2018). Cloning of the wheat *Yr15* resistance gene sheds light on the plant tandem kinase-pseudokinase family. *Nat. Commun.* 9(1), 3735. doi: 10.1038/s41467-018-06138-9.

Kuzay, S., Xu, Y., Zhang, J., Katz, A., Pearce, S., Su, Z., et al. (2019). Identification of a candidate gene for a QTL for spikelet number per spike on wheat chromosome arm 7AL by high-resolution genetic mapping. *Theor. Appl. Genet.* 132 (9), 2689-2705. doi: 10.1007/s00122-019-03382-5.

Li, C., Tang, H., Luo, W., Zhang, X., Mu, Y., Deng, M., et al. (2020). A novel, validated, and plant height-independent QTL for spike extension length is associated with yield-related traits in wheat. *Theor. Appl. Genet.* 133, 3381-3393. doi: 10.1007/s00122-020-03675-0.

Li, S., Jia, J., Wei, X., Zhang, X., Li, L., Chen, H., et al. (2007). A intervarietal genetic map and QTL analysis for yield traits in wheat. *Mol. Breed.* 20(2), 167-178. doi: 10.1007/s11032-007-9080-3.

Lin, Y., Chen, G., Hu, H., Yang, X., Zhang, Z., Jiang, X., et al. (2020). Phenotypic and genetic variation in phosphorus-deficiency-tolerance traits in Chinese wheat landraces. *BMC Plant Biol.* 20(1), 330. doi: 10.1186/s12870-020-02492-3.

Liu, H., Ma, J., Tu, Y., Zhu, J., Ding, P., Liu, J., et al. (2020a). Several stably expressed QTL for spike density of common wheat (*Triticum aestivum*) in multiple environments. *Plant Breed.* 139, 284-294. doi: 10.1111/pbr.12782.

Liu, J., Luo, W., Qin, N., Ding, P., Zhang, H., Yang, C., et al. (2018). A 55 K SNP array-based genetic map and its utilization in QTL mapping for productive tiller number in common wheat. *Theor. Appl. Genet.* 131(11), 2439-2450. doi: 10.1007/s00122-018-3164-9.

Liu, J., Tang, H., Qu, X., Liu, H., Li, C., Tu, Y., et al. (2020b). A novel, major, and validated QTL for the effective tiller number located on chromosome arm 1BL in bread wheat. *Plant Mol. Biol.* 104(1), 173-185. doi: 10.1007/s11103-020-01035-6.

Longin, C.F.H., and Reif, J.C. (2014). Redesigning the exploitation of wheat genetic resources. *Trends Plant Sci.* 19(10), 631-636. doi: 10.1016/j.tplants.2014.06.012.

Lopes, M.S., Ibrahim, E.B., Baenziger, P.S., Sukhwinder, S., Conxita, R., Kursad, O., et al. (2015). Exploiting genetic diversity from landraces in wheat breeding for adaptation to climate change. *J. Exp. Bot.* 66(12), 3477-3486. doi: 10.1093/jxb/erv122.

Luo, W., Ma, J., Zhou, X., Sun, M., Kong, X., Wei, Y., et al. (2016). Identification of quantitative trait loci controlling agronomic traits indicates breeding potential of Tibetan Semiwild Wheat (*Triticum aestivum* ssp. *tibetanum*). *Crop Sci.* 56, 2410-2420. doi: 10.2135/cropsci2015.11.0700.

Ma, J., Ding, P., Liu, J., Li, T., Zou, Y., Habib, A., et al. (2019a). Identification and validation of a major and stably expressed QTL for spikelet number per spike in bread wheat. *Theor. Appl. Genet.* 132(11), 3155-3167. doi: 10.1007/s00122-019-03415-z.

Ma, J., Qin, N., Cai, B., Chen, G., Ding, P., Zhang, H., et al. (2019b). Identification and validation of a novel major QTL for all-stage stripe rust resistance on 1BL in the winter wheat line 20828. *Theor. Appl. Genet.* 132(5), 1363-1373. doi: 10.1007/s00122-019-03283-7.

Ma, J., Tu, Y., Zhu, J., Luo, W., Liu, H., Li, C., et al. (2020). Flag leaf size and posture of bread wheat: genetic dissection, QTL validation and their relationships with yield-related traits. *Theor. Appl. Genet.* 133(1), 297-315. doi: 10.1007/s00122-019-03458-2.

Manickavelu, A., Kawaura, K., Imamura, H., Mori, M., and Ogihara, Y. (2011). Molecular mapping of quantitative trait loci for domestication traits and β-glucan content in a wheat recombinant inbred line population. *Euphytica* 177(2), 179-190. doi: 10.1007/s10681-010-0217-9.

Martínez-Moreno, F., Solís, I., Noguero, D., Blanco, A., Özberk, İ., Nsarellah, N., et al. (2020). Durum wheat in the Mediterranean Rim: historical evolution and genetic resources. *Genet. Resour. Crop. Evol.* 67, 1415-1436. doi: 10.1007/s10722-020-00913-8.

Miralles, D.J., Katz, S.D., Colloca, A., and Slafer, G.A. (1998). Floret development in near isogenic wheat lines differing in plant height. *Field Crop Res.* 59(1), 21-30. doi: 10.1016/S0378-4290(98)00103-8.

Mohler, V., Lukman, R., Ortiz-Islas, S., William, M., Worland, A.J., van Beem, J., et al. (2004). Genetic and physical mapping of photoperiod insensitive gene *Ppd-B1* in common wheat. *Euphytica* 138(1), 33-40. doi: 10.1023/B:EUPH.0000047056.58938.76.

Nelson, D.C., Lasswell, J., Rogg, L.E., Cohen, M.A., and Bartel, B. (2000). *FKF1*, a clock-controlled gene that regulates the transition to flowering in *Arabidopsis*. *Cell* 101, 331-340. doi: 10.1016/S0092-8674(00)80842-9.

Peng, J., Korol, A., Fahima, T., Roder, M., Li, Y., and Nevo, E. (2001). QTLs for agronomic traits in tetraploid wild emmer wheat, *Triticum dicoccoides*. *J. Sichuan Agric. Univ.* 19, 317-334. doi: 10.16036/j.issn.1000-2650.2001.04.005.

Quintero, A., Molero, G., Reynolds, M.P., and Calderini, D.F. (2018). Trade-off between grain weight and grain number in wheat depends on GxE interaction: A case study of an elite CIMMYT panel (CIMCOG). *Eur. J. Agron.* 92, 17-29. doi: 10.1016/j.eja.2017.09.007.

Rawson, H.M., and Richards, R.A. (1993). Effects of high temperature and photoperiod on floral development in wheat isolines differing in vernalisation and photoperiod genes. *Field Crop Res.* 32(3), 181-192. doi: 10.1016/0378-4290(93)90030-Q.

Ren, T., Hu, Y., Tang, Y., Li, C., Yan, B., Ren, Z., et al. (2018). Utilization of a wheat55K SNP array for mapping of major QTL for temporal expression of the tiller number. *Front. Plant Sci.* 9, 333. doi: 10.3389/fpls.2018.00333.

Reynolds, M., Bonnett, D., Chapman, S.C., Furbank, R.T., Manes, Y., Mather, D.E., et al. (2011). Raising yield potential of wheat. I. Overview of a consortium approach and breeding strategies. *J. Exp. Bot.* 62(2), 439-452. doi: 10.1093/jxb/erq311.

Sakuma, S., Golan, G., Guo, Z., Ogawa, T., Tagiri, A., Sugimoto, K., et al. (2019). Unleashing floret fertility in wheat through the mutation of a homeobox gene. *Proc. Natl. Acad. Sci. U. S. A.* 116, 5182-5187. doi: 10.1073/pnas.1815465116.

Samach, A., Klenz, J., Kohalmi, S., Risseeuw, E., Haughn, G., and Crosby, W. (1999). The *UNUSUAL FLORAL ORGANS* gene of *Arabidopsis thaliana* is an F-box protein required for normal patterning and growth in the floral meristem. *Plant J.* 20, 433-445. doi: 10.1046/j.1365-313x.1999.00617.x.

Shang, Q., Zhang, D., Li, R., Wang, K., Cheng, Z., Zhou, Z., et al. (2020). Mapping quantitative trait loci associated with stem-related traits in maize (*Zea mays* L.). *Plant Mol. Biol.* 104, 583-595. doi: 10.1007/s11103-020-01062-3.

Sharma, J.S., Running, K.L.D., Xu, S.S., Zhang, Q., Peters Haugrud, A.R., Sharma, S., et al. (2019). Genetic analysis of threshability and other spike traits in the evolution of cultivated emmer to fully domesticated durum wheat. *Mol. Genet. Genomics* 294(3), 757-771. doi: 10.1007/s00438-019-01544-0.

Shaw, L.M., Turner, A.S., Laurence, H., Simon, G., Laurie, D.A., and Somers, D.E. (2013). Mutant alleles of *Photoperiod-1* in wheat (*Triticum aestivum* L.) that confer a late flowering phenotype in long days. *PLoS One* 8(11), e79459. doi: 10.1371/journal.pone.0079459.

Sthapit, S.R., Marlowe, K., Covarrubias, D.C., Ruff, T.M., Eagle, J.D., McGinty, E.M., et al. (2020). Genetic diversity in historical and modern wheat varieties of the U.S. Pacific Northwest. *Crop Sci.* 60, 3175-3190. doi: 10.1002/csc2.20299.

Tanksley, S.D., and McCouch, S.R. (1997). Seed banks and molecular maps: unlocking genetic potential from the wild. *Science* 277(5329), 1063-1066. doi: 10.1126/science.277.5329.1063.

Tao, Y., Yi, X., Lin, Y., Wang, Z., Wu, F., Jiang, X., et al. (2019). Quantitative trait locus mapping for panicle exsertion length in common wheat using two related recombinant inbred line populations. *Euphytica* 215(6), 104. doi: 10.1007/s10681-019-2433-2.

Tu, Y., Liu, H., Liu, J., Tang, H., Mu, Y., Deng, M., et al. (2021). QTL mapping and validation of bread wheat flag leaf morphology across multiple environments in different genetic backgrounds. *Theor. Appl. Genet.* 134(1), 261-278. doi: 10.1007/s00122-020-03695-w.

Walker, J.C. (2010). Receptor-like protein kinase genes of *Arabidopsis thaliana*. *Plant J.* 3(3), 451-456. doi: 10.1046/j.1365-313X.1993.t01-23-00999.x.

Wang, R., Liu, Y., Isham, K., Zhao, W., Wheeler, J., Klassen, N., et al. (2018). QTL identification and KASP marker development for productive tiller and fertile spikelet numbers in two high-yielding hard white spring wheat cultivars. *Mol. Breed.* 38(11), 135. doi: 10.1007/s11032-018-0894-y.

Wang, Y., Yu, H., Tian, C., Sajjad, M., Gao, C., Tong, Y., et al. (2017). Transcriptome association identifies regulators of wheat spike architecture. *Plant Physiol.* 175(2), 746-757. doi: 10.1104/pp.17.00694.

Wu, X., Chang, X., and Jing, R. (2012). Genetic insight into yield-associated traits of wheat grown in multiple rain-fed environments. *PloS One* 7, e31249. doi: 10.1371/journal.pone.0031249.

Xie, Q., Sean, M., and Sparkes, D.L. (2015). Spelt as a genetic resource for yield component improvement in bread wheat. *Crop Sci.* 55(6), 2753-2765. doi: 10.2135/cropsci2014.12.0842.

Xie, W., and Nevo, E. (2008). Wild emmer: genetic resources, gene mapping and potential for wheat improvement. *Euphytica* 164(3), 603-614. doi: 10.1007/s10681-008-9703-8.

Xu, X., Zhang, X., Shi, Y., Wang, H., Feng, B., Li, X., et al. (2016). A point mutation in an F-box domain-containing protein is responsible for brown hull phenotype in rice. *Rice Sci.* 23(1), 1-8. doi: 10.1016/j.rsci.2016.01.001.

Yao, H., Xie, Q., Xue, S., Luo, J., Lu, J., Kong, Z., et al. (2019). *HL2* on chromosome 7D of wheat (*Triticum aestivum* L.) regulates both head length and spikelet number. *Theor. Appl. Genet.* 132(6), 1789-1797. doi: 10.1007/s00122-019-03315-2.

Yao, J., Ren, L., Zhang, P., Yang, X., and Zhou, M. (2011). Genetic and correlation analysis of plant height and its components in wheat. *J. Triticeae Crop* 31, 604-610 (in Chinese with English abstract).

Yu, J., Zhao, Y., Ding, M., Yu, Z., Jiang, Y., Ma, W., et al. (2020). Wild emmer chromosome arm substitution lines: Useful resources for wheat genetic study and breeding. *Crop Sci.* 60, 1761-1769. doi: 10.1002/csc2.20022.

Zhang, H., Li, Y., Miao, L., Wang, J., Li, C., Yang, D., et al. (2019). Transcription factor gene *TaNAC67* involved in regulation spike length and spikelet number per spike in common wheat. *Acta Agron. Sin.* 45(11), 1615-1627 (in Chinese with English abstract). doi: 10.3724/sp.J.1006.2019.91009.

Zhang, K., Xu, X., and Tian, J. (2009). QTL mapping for grain yield and spike related traits in common wheat. *Acta Agron. Sin.* 35(2), 270-278 (in Chinese with English abstract). doi: 10.3724/SP.J.1006.2009.00270

**Table 1** Information of SNP markers in the genetic map

| Chromosome | Group | Number of bin marker | Number of mapped marker | Length (cM) | cM per bin marker |
|---|---|---|---|---|---|
| 1A | 1 | 101 | 586 | 153.29 | 1.52 |
| 1B | 1 | 69 | 488 | 149.34 | 2.16 |
| 2A | 1 | 66 | 944 | 161.77 | 2.45 |
| 2B | 1 | 92 | 423 | 183.69 | 2.00 |
| 3A | 1 | 99 | 518 | 160.97 | 1.63 |
| 3B | 1 | 17 | 37 | 49.69 | 2.92 |
| | 2 | 27 | 174 | 98.39 | 3.64 |
| 4A | 1 | 80 | 282 | 199.90 | 2.50 |
| 4B | 1 | 77 | 422 | 83.69 | 1.09 |
| 5A | 1 | 92 | 299 | 225.06 | 2.45 |
| 5B | 1 | 121 | 675 | 207.52 | 1.72 |
| 6A | 1 | 60 | 640 | 167.00 | 2.78 |
| 6B | 1 | 58 | 160 | 162.46 | 2.80 |
| 7A | 1 | 92 | 395 | 214.20 | 2.33 |
| 7B | 1 | 99 | 499 | 194.81 | 1.97 |
| A genome | 7 | 590 | 3664 | 1282.19 | 2.17 |
| B genome | 8 | 560 | 2878 | 1129.59 | 2.02 |
| Total | 15 | 1150 | 6542 | 2411.78 | 2.10 |

**Table 2** Phenotypic data and heritability ($H^2$) of spikelet number per spike (SNS) for the AM population in multiple environments

| Environment | Parents | | AL × LM001 (AM) | | | |
|---|---|---|---|---|---|---|
| | AL | LM001 | Min-Max | Mean | SD | $H^2$ |
| $E_1$ | 25.00 | 24.33 | 20.00-31.67 | 25.96 | 2.56 | |
| $E_2$ | 26.00 | 23.33 | 15.33-33.00 | 24.41 | 3.22 | |
| $E_3$ | 26.33 | 26.00 | 17.00-31.25 | 24.81 | 2.80 | |
| $E_4$ | 26.00 | 25.40 | 18.00-32.00 | 26.21 | 2.87 | |
| $E_5$ | 27.00 | 24.60 | 18.50-31.00 | 24.99 | 2.42 | |
| $E_6$ | 25.80 | 25.40 | 20.00-34.00 | 26.76 | 2.69 | |
| BLUP | 25.98 | 24.91 | 18.89-30.54 | 25.53 | 2.09 | 0.82 |

*BLUP* phenotype values based on the best linear unbiased prediction, *SD* standard deviation, $H^2$ the broad-sense heritability

**Table 3** Correlations of spikelet number per spike (SNS) in the AM population between six environments

| | $E_1$ | $E_2$ | $E_3$ | $E_4$ | $E_5$ | $E_6$ |
|---|---|---|---|---|---|---|
| $E_1$ | 1 | 0.500** | 0.619** | 0.645** | 0.521** | 0.534** |
| $E_2$ | | 1 | 0.666** | 0.631** | 0.626** | 0.648** |
| $E_3$ | | | 1 | 0.704** | 0.672** | 0.622** |
| $E_4$ | | | | 1 | 0.761** | 0.616** |
| $E_5$ | | | | | 1 | 0.662** |
| $E_6$ | | | | | | 1 |

**Significance level at $P < 0.01$

**Table 4** Correlations between spikelet number per spike (SNS) and other agronomic traits in the AM population

| | SNS |
|---|---|
| PH | 0.320** |
| AD | 0.179* |
| PTN | -0.099 |
| SL | 0.686** |
| SEL | 0.241** |
| KNS | 0.423** |
| KNL | 0.014 |
| SD | 0.274** |
| TKW | 0.198* |

*PH* plant height, *AD* anthesis date, *PTN* productive tiller number, *SL* spike length, *SEL* spike extension length, *KNS* kernel number per spike, *KNL* kernel number per spikelet, *SD* spike density, *TKW* thousand kernel weight. *Significance level at $P < 0.05$, **Significance level at $P < 0.01$

**Table 5** Quantitative trait loci (QTL) for spikelet number per spike (SNS) identified in multiple environments in the AM population

| QTL | Env. | Interval (cM) | Left Marker | Right Marker | LOD | PVE (%) | Add |
|---|---|---|---|---|---|---|---|
| *QSns.sau-AM-1A* | $E_2$ | 148.47-153.29 | *AX-110167459* | *AX-110373055* | 6.73 | 14.73 | -1.31 |
| *QSns.sau-AM-3A* | $E_4$ | 79.51-91.05 | *AX-109418113* | *AX-109284498* | 3.03 | 6.91 | 0.69 |
| *QSns.sau-AM-5A.1* | $E_2$ | 106.81-107.24 | *AX-110428951* | *AX-109898601* | 3.26 | 6.11 | -0.85 |
| *QSns.sau-AM-5A.2* | $E_1$ | 116.08-131.93 | *AX-108790581* | *AX-111499991* | 4.78 | 14.34 | -1.02 |
| | $E_3$ | 131.93-135.18 | *AX-111499991* | *AX-111596791* | 3.17 | 6.69 | -0.74 |
| | BLUP | 131.93-135.18 | *AX-111499991* | *AX-111596791* | 6.09 | 10.28 | -0.67 |
| *QSns.sau-AM-6A* | $E_2$ | 91.51-92.38 | *AX-109842268* | *AX-108785002* | 3.38 | 6.62 | 0.87 |
| *QSns.sau-AM-2B.1* | $E_4$ | 92.48-94.75 | *AX-109818835* | *AX-108848446* | 3.91 | 9.31 | -0.80 |
| *QSns.sau-AM-2B.2* | $E_5$ | 113.67-114.56 | *AX-109421413* | *AX-109506426* | 3.81 | 12.71 | -0.74 |
| *QSns.sau-AM-2B.3* | $E_1$ | 127.65-129.44 | *AX-111626925* | *AX-111588559* | 8.19 | 20.27 | -1.21 |
| | $E_2$ | 127.65-129.44 | *AX-111626925* | *AX-111588559* | 5.00 | 9.64 | -1.04 |
| | $E_3$ | 127.65-129.44 | *AX-111626925* | *AX-111588559* | 10.86 | 27.26 | -1.49 |
| | $E_4$ | 127.65-129.44 | *AX-111626925* | *AX-111588559* | 5.71 | 14.16 | -0.98 |
| | $E_5$ | 127.65-129.44 | *AX-111626925* | *AX-111588559* | 5.88 | 20.77 | -0.93 |
| | $E_6$ | 127.65-129.44 | *AX-111626925* | *AX-111588559* | 4.54 | 13.90 | -0.95 |
| | BLUP | 127.65-129.44 | *AX-111626925* | *AX-111588559* | 13.28 | 26.50 | -1.07 |
| *QSns.sau-AM-3B.1* | $E_4$ | 22.72-42.47 | *AX-110399975* | *AX-109050064* | 6.36 | 18.06 | 1.14 |
| | $E_6$ | 22.72-42.47 | *AX-110399975* | *AX-109050064* | 3.11 | 9.38 | 0.81 |
| *QSns.sau-AM-3B.2* | $E_1$ | 48.34-49.69 | *AX-109393346* | *AX-110548993* | 4.13 | 9.57 | 0.85 |
| | $E_2$ | 48.34-49.69 | *AX-109393346* | *AX-110548993* | 4.89 | 9.32 | 1.05 |
| | $E_3$ | 48.34-49.69 | *AX-109393346* | *AX-110548993* | 5.28 | 11.82 | 1.00 |
| | $E_5$ | 48.34-49.69 | *AX-109393346* | *AX-110548993* | 2.53 | 8.27 | 0.60 |
| | BLUP | 48.34-49.69 | *AX-109393346* | *AX-110548993* | 7.81 | 13.74 | 0.79 |
| *QSns.sau-AM-4B* | $E_2$ | 68.66-69.11 | *AX-111151524* | *AX-109338618* | 4.13 | 7.82 | 0.96 |
| *QSns.sau-AM-5B.1* | BLUP | 131.85-133.16 | *AX-110547223* | *AX-108834482* | 3.93 | 6.38 | 0.53 |
| *QSns.sau-AM-5B.2* | $E_4$ | 142.38-143.74 | *AX-110911600* | *AX-109870696* | 2.81 | 6.41 | 0.66 |
| *QSns.sau-AM-6B* | BLUP | 123.88-124.75 | *AX-108748222* | *AX-86183685* | 2.67 | 4.23 | 0.43 |

*Env.* Environment, *BLUP* phenotype values based on the best linear unbiased prediction, *LOD* logarithm of odds, *PVE* phenotype variance explained, *Add* additive effect, positive values: alleles from AL were increasing the trait score, negative values: alleles from LM001 were increasing the score

**Figure Legends**

**Figure. 1** The spikes of AL and LM001 (scale bar = 2 cm)

**Figure. 2** Distribution information of 1150 bin markers on the genetic maps. The positions of centromeres were indicated by yellow areas and black arrows. The short arms (blue) and long arms (red) of chromosomes were in the upper and lower parts, respectively. The markers were black indicated that their physical locations were not on the corresponding chromosomes. The names of bin markers were listed on the right side of the chromosomes

**Figure. 3** The syntenic relationships between the genetic and physical maps of bin markers (excluding the 49 bin markers of unknown chromosomes). Gen-1A to Gen-7B represented the 15 chromosomal genetic maps used in the current study; Phy-1A to Phy-7B represented the 14 chromosomal physical maps of wild emmer genome

**Figure. 4** AM RILs were divided into two categories based on the genotype of flanking markers, and the SNS differences caused by the corresponding QTL were represented in the form of boxplots. Genetic maps of *QSns.sau-AM-5A.2* (**a**), *QSns.sau-AM-2B.3* (**b**), *QSns.sau-AM-3B.1* (**c**), *QSns.sau-AM-3B.2* (**d**) and their effects. *Significance level at $P < 0.05$, **Significance level at $P < 0.01$. The SNS differences between the two categories were marked below the environment names

**Figure. 5** The individual and cumulative effects of *QSns.sau-AM-2B.3* and *QSns.sau-AM-3B.2* on increasing SNS in the AM population. '+' and '-' represented lines with and without the positive allele of the corresponding QTL based on the genotype of flanking markers, respectively. *Significance level at $P < 0.05$, **Significance level at $P < 0.01$

**Figure. 6** Student's *t*-test against the two categories of lines from the AM RIL population possessing the positive or negative alleles of both *QSns.sau-AM-2B.3* and

*QSns.sau-AM-3B.2* for (**a**) plant height (PH); (**b**) anthesis date (AD); (**c**) productive tiller number (PTN); (**d**) spike length (SL); (**e**) spike extension length (SEL); (**f**) kernel number per spike (KNS); (**g**) kernel number per spikelet (KNL); (**h**) spike density (SD); (**i**) thousand kernel weight (TKW). *Significance level at $P < 0.05$, **Significance level at $P < 0.01$. Differences between the two categories of lines were marked above the significance levels

**Figure. 7** The physical intervals of *QSns.sau-AM-2B.3* (**a**) and *QSns.sau-AM-3B.2* (**b**)

**Supplementary Materials**

**Supplementary Table 1** Environmental information of surveyed agronomic traits

**Supplementary Table 2** The 1150 bin markers used for QTL mapping

**Supplementary Table 3** Comparison of the genetic and physical positions of 6542 mapped markers (including bin markers and co-segregated markers)

**Supplementary Table 4** Quantitative trait loci (QTL) detected in the QTL-by-Environment interaction module

**Supplementary Table 5** Quantitative trait loci (QTL) detected in additional spike-related traits

**Supplementary Table 6** Comparison of *QSns.sau-AM-2B.3* and *QSns.sau-AM-3B.2* with previously reported quantitative trait loci (QTL) for spikelet number per spike (SNS) on chromosome 2B and 3B, respectively

**Supplementary Table 7** Predicted genes in the physical interval of the major QTL *QSns.sau-AM-2B.3*

**Supplementary Table 8** Predicted genes in the physical interval of the major QTL

*QSns.sau-AM-3B.2*

**Supplementary Figure 1** The syntenic relationships of mapped markers between genetic and physical positions. Excluding 125 markers that had unknown physical chromosomal locations and 213 markers which had inconsistent chromosomal locations between genetic and physical maps. Gen-1A to Gen-7B represented the 15 genetic maps used in the current study; Phy-1A to Phy-7B represented the 14 physical maps of wild emmer genome

**Supplementary Figure 2** Frequency distributions of SNS in the AM population from six environments and BLUP. Solid and dotted arrows represented AL and LM001, respectively

AL
LM001

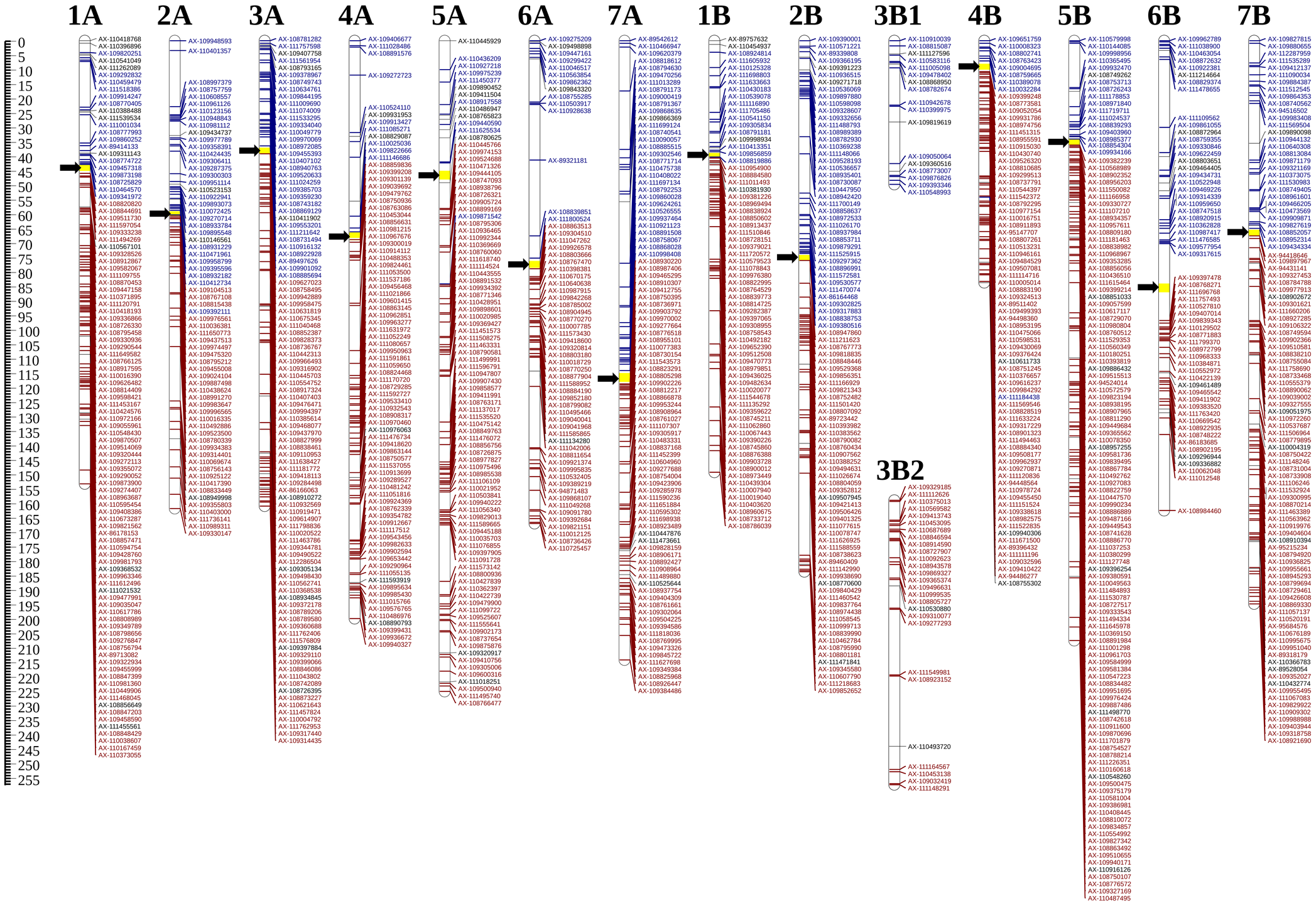
1A
2A
3A
4A
5A
6A
7A
1B
2B
3B1
4B
5B
6B
7B
3B2

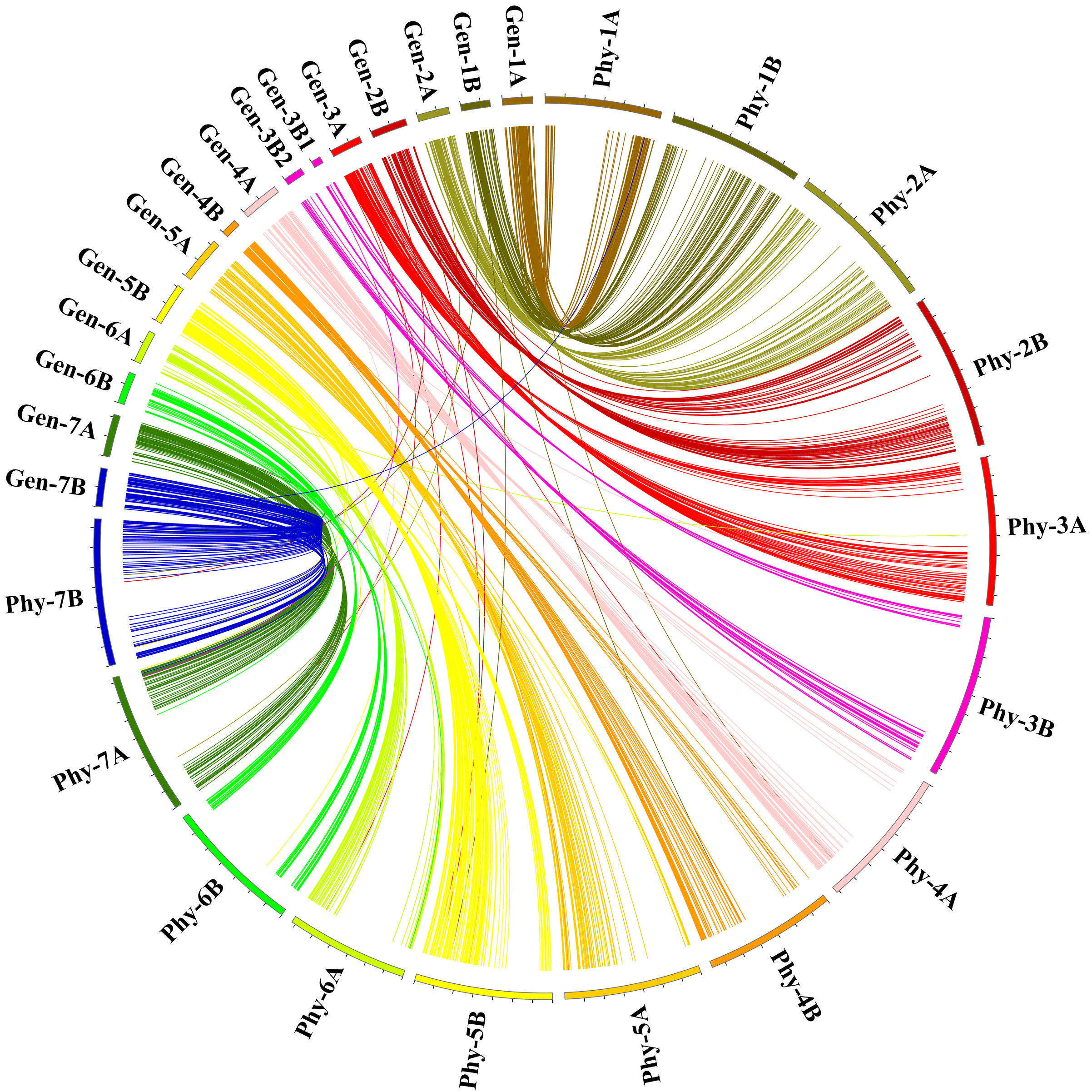
Gen-1A
Gen-1B
Gen-2A
Gen-2B
Gen-3A
Gen-3B1
Gen-3B2
Gen-4A
Gen-4B
Gen-5A
Gen-5B
Gen-6A
Gen-6B
Gen-7A
Gen-7B
Phy-1A
Phy-1B
Phy-2A
Phy-2B
Phy-3A
Phy-3B
Phy-4A
Phy-4B
Phy-5A
Phy-5B
Phy-6A
Phy-6B
Phy-7A
Phy-7B

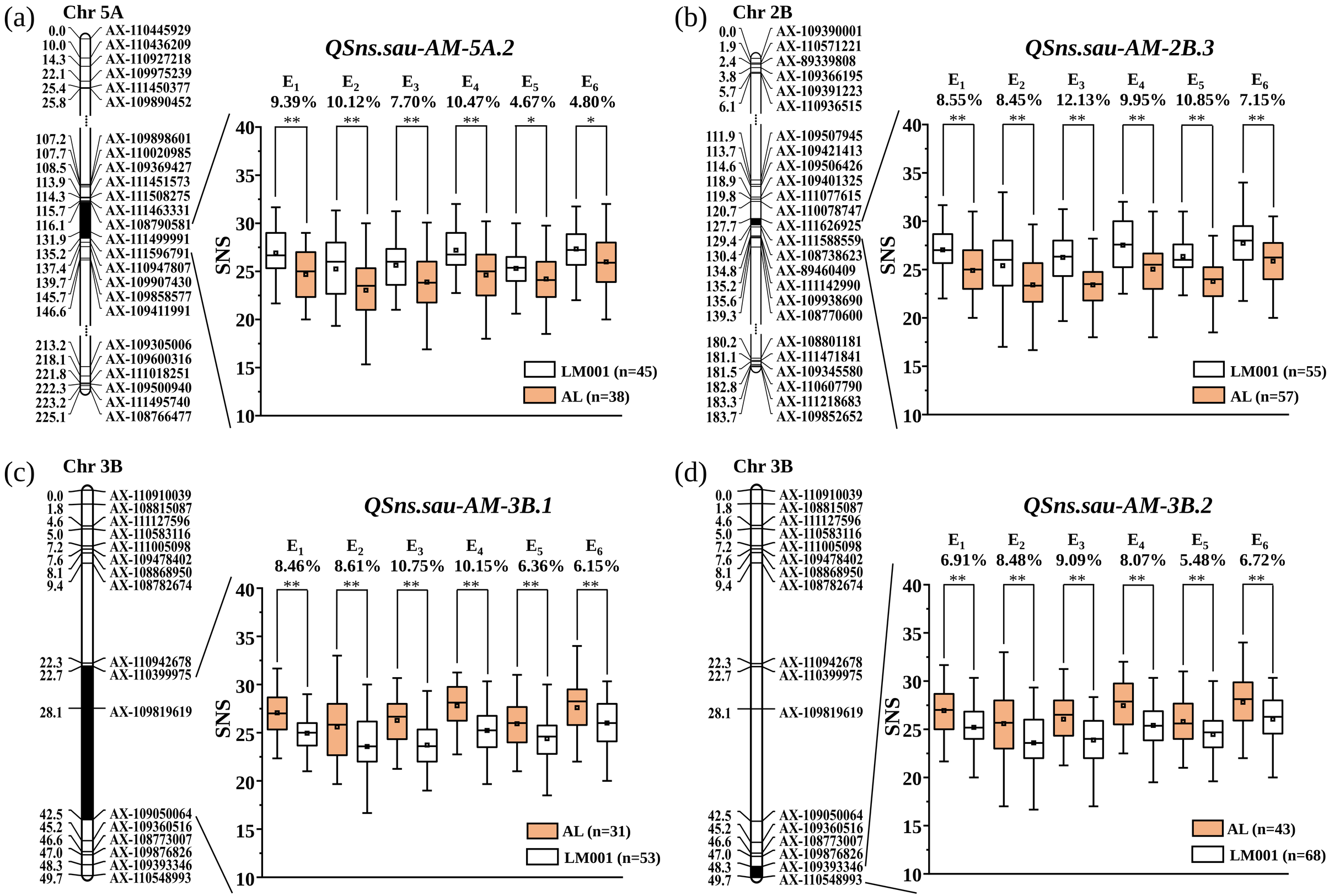
(a)
Chr 5A
0.0 AX-110445929
10.0 AX-110436209
14.3 AX-110927218
22.1 AX-109975239
25.4 AX-111450377
25.8 AX-109890452
107.2 AX-109898601
107.7 AX-110020985
108.5 AX-109369427
113.9 AX-111451573
114.3 AX-111508275
115.7 AX-111463331
116.1 AX-108790581
131.9 AX-111499991
135.2 AX-111596791
137.4 AX-110947807
139.7 AX-109907430
145.7 AX-109858577
146.6 AX-109411991
213.2 AX-109305006
218.1 AX-109600316
221.8 AX-111018251
222.3 AX-109500940
223.2 AX-111495740
225.1 AX-108766477
QSns.sau-AM-5A.2
E1 9.39% E2 10.12% E3 7.70% E4 10.47% E5 4.67% E6 4.80%
SNS
LM001 (n=45)
AL (n=38)
(b)
Chr 2B
0.0 AX-109390001
1.9 AX-110571221
2.4 AX-89339808
3.8 AX-109366195
5.7 AX-109391223
6.1 AX-110936515
111.9 AX-109507945
113.7 AX-109421413
114.6 AX-109506426
118.9 AX-109401325
119.8 AX-111077615
120.7 AX-110078747
127.7 AX-111626925
129.4 AX-111588559
130.4 AX-108738623
134.8 AX-89460409
135.2 AX-111142990
135.6 AX-109938690
139.3 AX-108770600
180.2 AX-108801181
181.1 AX-111471841
181.5 AX-109345580
182.8 AX-110607790
183.3 AX-111218683
183.7 AX-109852652
QSns.sau-AM-2B.3
E1 8.55% E2 8.45% E3 12.13% E4 9.95% E5 10.85% E6 7.15%
SNS
LM001 (n=55)
AL (n=57)
(c)
Chr 3B
0.0 AX-110910039
1.8 AX-108815087
4.6 AX-111127596
5.0 AX-110583116
7.2 AX-111005098
7.6 AX-109478402
8.1 AX-108868950
9.4 AX-108782674
22.3 AX-110942678
22.7 AX-110399975
28.1 AX-109819619
42.5 AX-109050064
45.2 AX-109360516
46.6 AX-108773007
47.0 AX-109876826
48.3 AX-109393346
49.7 AX-110548993
QSns.sau-AM-3B.1
E1 8.46% E2 8.61% E3 10.75% E4 10.15% E5 6.36% E6 6.15%
SNS
AL (n=31)
LM001 (n=53)
(d)
Chr 3B
0.0 AX-110910039
1.8 AX-108815087
4.6 AX-111127596
5.0 AX-110583116
7.2 AX-111005098
7.6 AX-109478402
8.1 AX-108868950
9.4 AX-108782674
22.3 AX-110942678
22.7 AX-110399975
28.1 AX-109819619
42.5 AX-109050064
45.2 AX-109360516
46.6 AX-108773007
47.0 AX-109876826
48.3 AX-109393346
49.7 AX-110548993
QSns.sau-AM-3B.2
E1 6.91% E2 8.48% E3 9.09% E4 8.07% E5 5.48% E6 6.72%
SNS
AL (n=43)
LM001 (n=68)

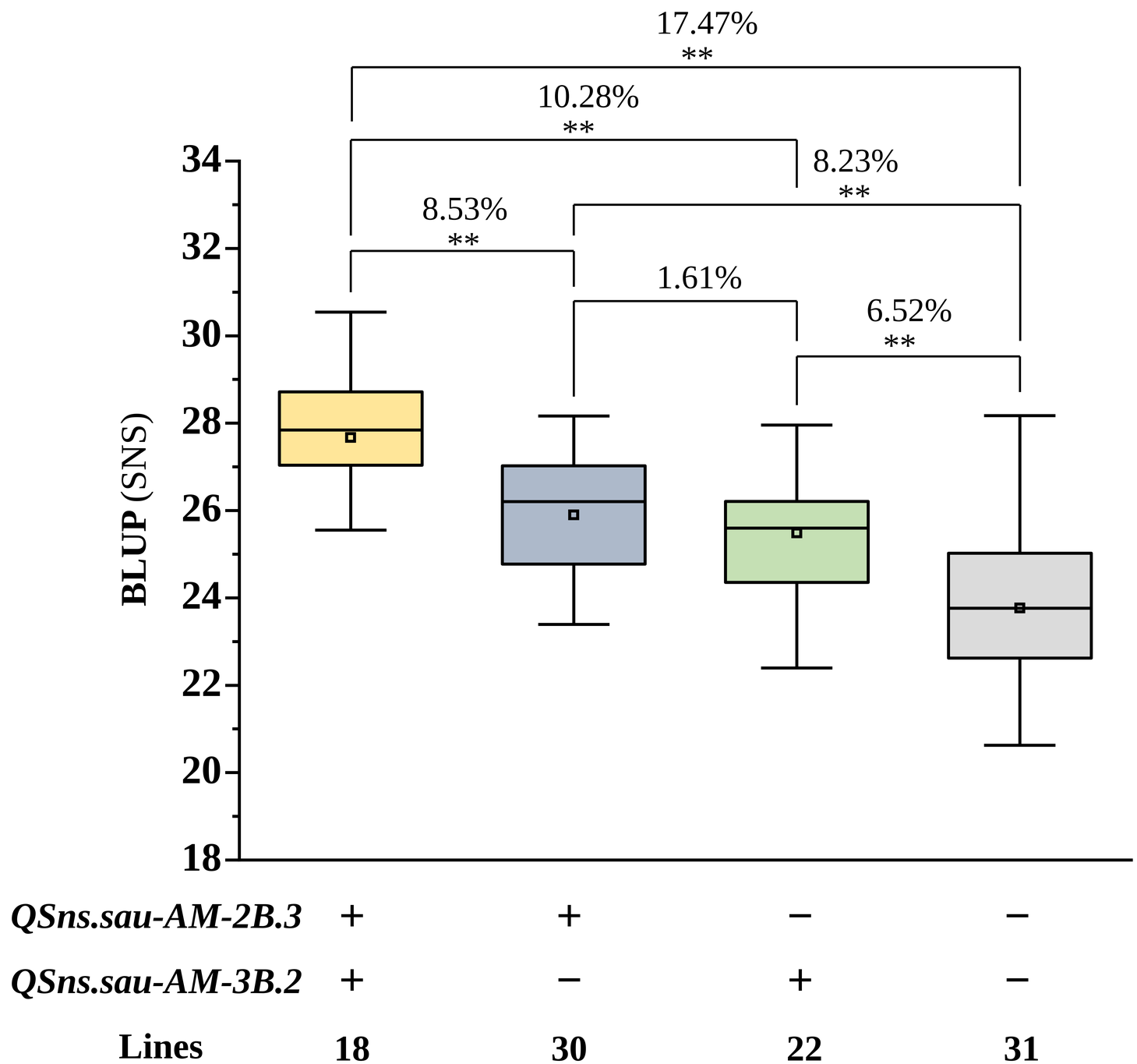
17.47%
**
10.28%
**
8.23%
**
8.53%
**
1.61%
6.52%
**
BLUP (SNS)
34
32
30
28
26
24
22
20
18
QSns.sau-AM-2B.3 + + − −
QSns.sau-AM-3B.2 + − + −
Lines 18 30 22 31

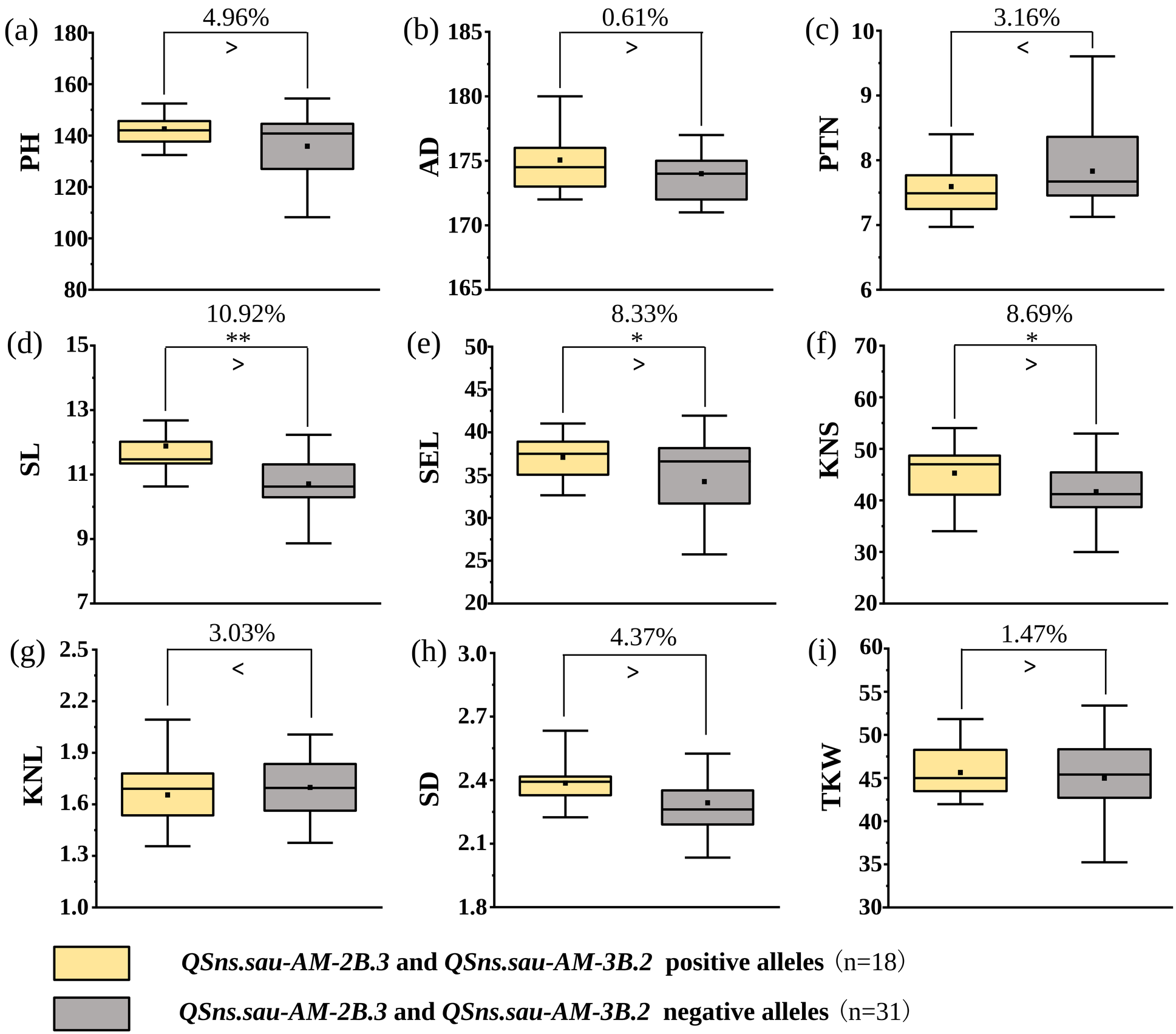
(a)
4.96%
>
PH
180
160
140
120
100
80
(b)
0.61%
>
AD
185
180
175
170
165
(c)
3.16%
<
PTN
10
9
8
7
6
(d)
10.92%
**
>
SL
15
13
11
9
7
(e)
8.33%
*
>
SEL
50
45
40
35
30
25
20
(f)
8.69%
*
>
KNS
70
60
50
40
30
20
(g)
3.03%
<
KNL
2.5
2.2
1.9
1.6
1.3
1.0
(h)
4.37%
>
SD
3.0
2.7
2.4
2.1
1.8
(i)
1.47%
>
TKW
60
55
50
45
40
35
30
QSns.sau-AM-2B.3 and QSns.sau-AM-3B.2 positive alleles（n=18）
QSns.sau-AM-2B.3 and QSns.sau-AM-3B.2 negative alleles（n=31）

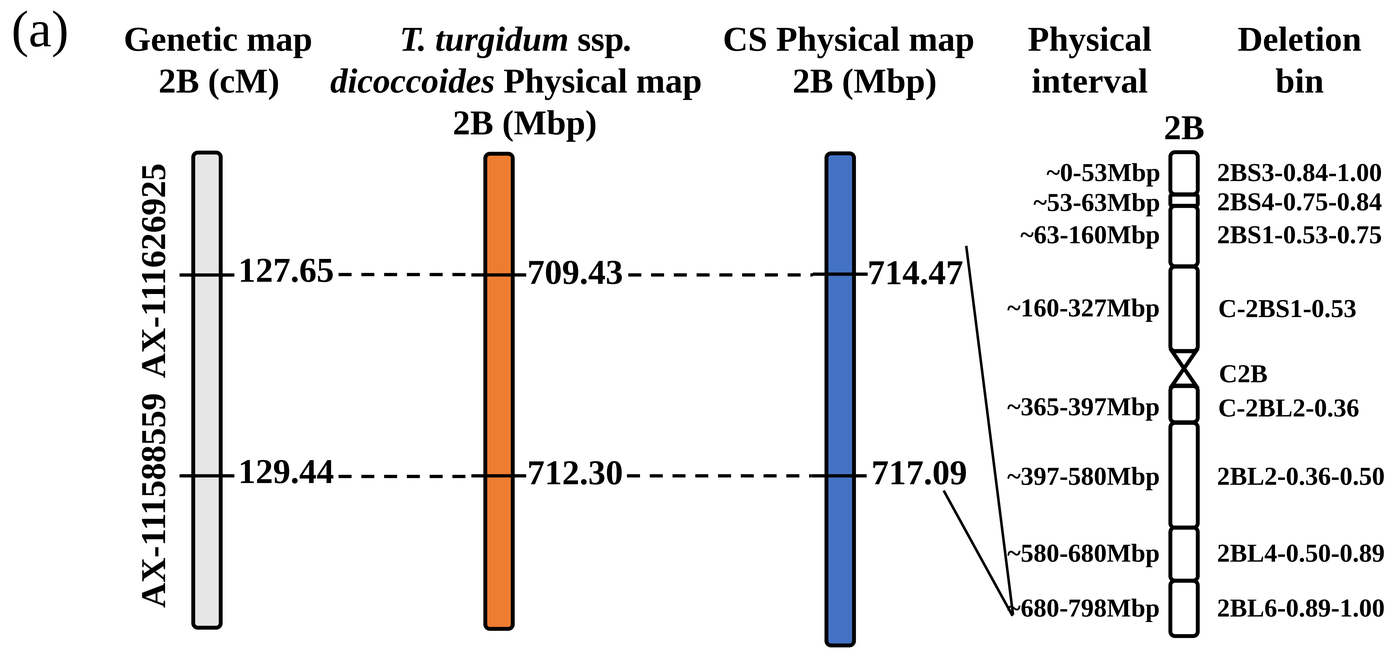
(a)
Genetic map 2B (cM)
T. turgidum ssp. dicoccoides Physical map 2B (Mbp)
CS Physical map 2B (Mbp)
Physical interval
Deletion bin
2B
AX-11626925
AX-11588559
127.65
709.43
714.47
129.44
712.30
717.09
~0-53Mbp
~53-63Mbp
~63-160Mbp
~160-327Mbp
~365-397Mbp
~397-580Mbp
~580-680Mbp
~680-798Mbp
2BS3-0.84-1.00
2BS4-0.75-0.84
2BS1-0.53-0.75
C-2BS1-0.53
C2B
C-2BL2-0.36
2BL2-0.36-0.50
2BL4-0.50-0.89
2BL6-0.89-1.00

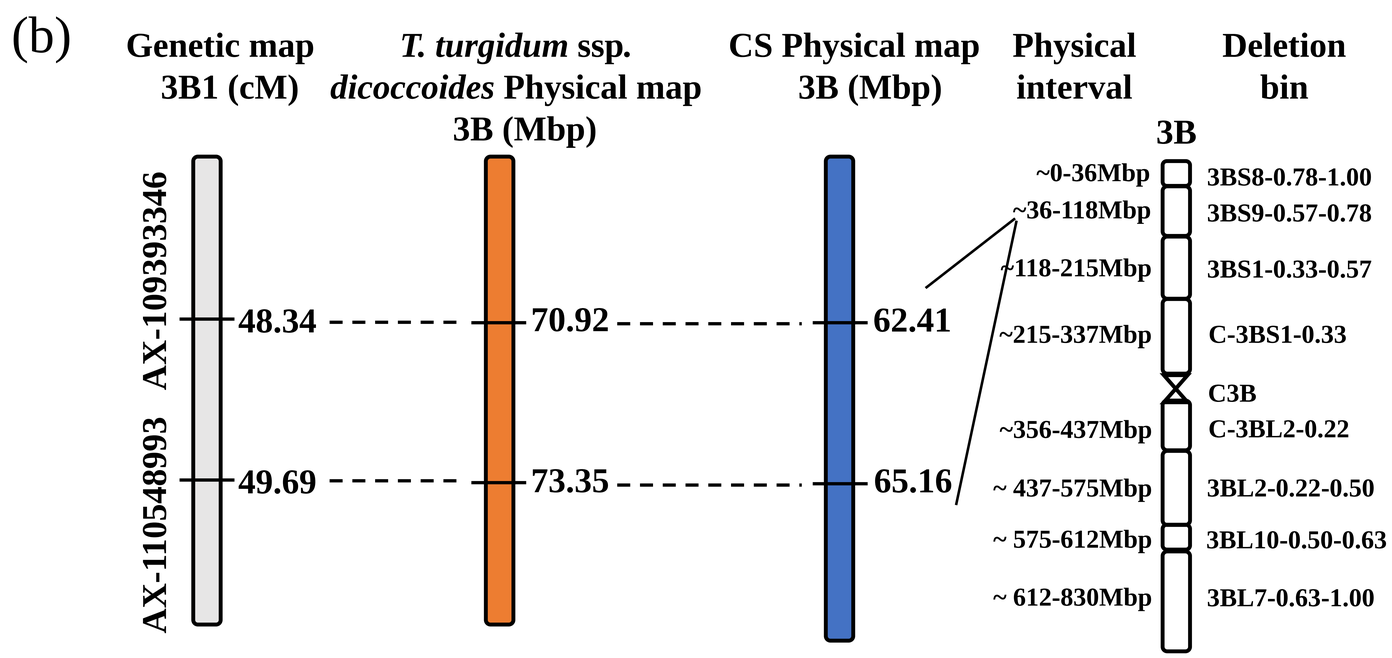
(b)
Genetic map 3B1 (cM)
T. turgidum ssp. dicoccoides Physical map 3B (Mbp)
CS Physical map 3B (Mbp)
Physical interval
Deletion bin
3B
AX-109393346
AX-110548993
48.34
70.92
62.41
49.69
73.35
65.16
~0-36Mbp
~36-118Mbp
~118-215Mbp
~215-337Mbp
~356-437Mbp
~ 437-575Mbp
~ 575-612Mbp
~ 612-830Mbp
3BS8-0.78-1.00
3BS9-0.57-0.78
3BS1-0.33-0.57
C-3BS1-0.33
C3B
C-3BL2-0.22
3BL2-0.22-0.50
3BL10-0.50-0.63
3BL7-0.63-1.00